

Characterization of the Piezochromic Behavior of Some Members of the $\text{CuMo}_{1-x}\text{W}_x\text{O}_4$ Series

M. Gaudon,^{*,†} A. E. Thiry,^{†,‡} A. Largeteau,[†] P. Deniard,[‡] S. Jobic,[‡] J. Majimel,[†] and A. Demourgues[†]

Institut de Chimie de la Matière Condensée de Bordeaux, 87 Avenue du Docteur Schweitzer, 33608 PESSAC Cedex, France, and Institut des Matériaux Jean Rouxel, UMR 6502 CNRS-Université de Nantes, BP 32229, 44322 Nantes Cedex 3, France

Received August 30, 2007

The members of the $\text{CuMo}_{1-x}\text{W}_x\text{O}_4$ series ($0 \leq x < 0.1$) undergo a first-order phase transition that can be induced by pressure application; the thermochromic properties of such a series have already been reported. The two polymorphic forms exhibit two distinguishable colors: green for the low pressure form (α) and brownish-red for the high pressure one (γ). These oxides can open up a new market for friendly pressure indicators, particularly for the compositions ($0.07 \leq x \leq 0.1$) for which the two polymorphs are stable at room temperature, that is, for which the color transition via pressure application is nonreversible. Within the $\text{CuMo}_{1-x}\text{W}_x\text{O}_4$ solid solution domain, the dependence of the transition pressure versus tungsten content, temperature of measurement, and sample thermal-pressure history was studied. A large control of the transition pressure (from 5 to several 100 MPa) was brought to the fore. The transition was then studied using X-ray diffraction and transmission electron microscopy-energy dispersive X-ray analyses. This first-order transition, occurring by atomic migration inside the cell, seems to be preceded by an atomic disordering; moreover, transition temperatures may be modified by W segregation at the surface of the grains.

Introduction

Currently, piezochromic compounds with well defined transition pressure attract tremendous interest because of their potential applications as shock detectors, security inks (to fight against counterfeiting), and user-friendly materials in cosmetic creams and smart paints, for instance. Piezochromic materials (sometimes reported as tribochromic materials) can be defined as materials presenting a reversible or irreversible change in their coloration with pressure, this change occurring progressively or suddenly around the transition pressure. For suitable applications in everyday life, the applied transition pressure should be relatively low and should correspond, for example, to that of a human finger push. From our knowledge, such a material with a significant color change at the transition does not exist nowadays. In fact, tribo/piezochromic behaviors are mainly reported in the literature for very high pressure, that is, above one GPa (see

refs 1–4 for very recent examples). In particular, wurtzite to NaCl-type transitions were intensively studied. For illustration, CdS exhibits a change of coloration from yellow to red during the wurtzite to NaCl-type phase transition which takes place at about 2.5 GPa.⁴ Promising systems for suitable applications are the CuMoO_4 oxide and its W derivatives which exhibit both thermochromic and piezochromic properties. The end member of the series, CuMoO_4 , exhibits a phase transition around 250 MPa^{5–7} which severely limits its use in the industry. Nevertheless, a part of the molybdenum cations in CuMoO_4 can be substituted for tungsten ones to tune the transition temperatures or transition pressures of

* To who correspondence should be addressed. E-mail: gaudon@icmcb-bordeaux.cnrs.fr.

[†] Institut de Chimie de la Matière Condensée de Bordeaux.

[‡] Université de Nantes.

- (1) Ehm, L.; Knorr, K.; Peters, L.; Rath, S.; Depmeier, W. *J. Alloys Compd.* **2007**, *429*, 82–86.
- (2) Balog, P.; Orosel, D.; Cancarevic, Z.; Schön, C.; Jansen, M. *J. Alloys Compd.* **2007**, *429*, 87–98.
- (3) Xiang-Rong, C.; Xiao-Feng, L.; Ling-Cang, C.; Jun, Z. *Solid State Commun.* **2006**, *139*, 246–249.
- (4) Sowa, H. *Solid State Sci.* **2005**, *7*, 73–78.
- (5) Rodríguez, D.; Hernández, J.; Garcia-Jaca, H.; Ehrenberg, H.; Weitzel, H. *Physica B (Amsterdam)* **1999**, *265*, 181–185.
- (6) Wiesmann, M.; Ehrenberg, H.; Miehe, G.; Peun, T.; Weitzel, H.; Fuess, H. *J. Solid State Chem.* **1997**, *132*, 88–97.
- (7) Ehrenberg, H.; Weitzel, H.; Paulus, H.; Wiesmann, M.; Wltschek, G.; Geselle, M.; Fuess, H. *J. Phys. Chem. Solids* **1997**, *58*, 153–160.

thermochromic/piezochromic phenomena.^{7,8} In $\text{CuMo}_{1-x}\text{W}_x\text{O}_4$ ($x \leq 0.1$) compounds, the green to red change in coloration is associated with a pressure induced structural phase transition from the α -form to the γ -form without modification of the space group. This first-order transition goes along with a large change in the compound volume of about 11–12%. In a first publication⁹ on the $\text{CuMo}_{1-x}\text{W}_x\text{O}_4$ series, the transition temperatures were characterized with several techniques such as superconducting quantum interference device (SQUID) measurements, differential scanning calorimetry (DSC), and temperature reflectivity in the visible range. It was shown that the thermochromic transition temperatures can be controlled by the tungsten rate in the oxides (x) in the limit of the solubility domain. Thus, transition temperatures can vary in a large range from -80 °C over 100 °C under cooling or heating with a hysteresis loop of about 100 °C.

In this paper, we report on the influence of the tungsten rate and the thermal/pressure history of the samples on their piezochromic properties. Typically, high isostatic pressures were applied from oxygen media in appropriate vessels, and the transition pressure was then extracted from colorimetric parameters curves obtained by diffuse reflectance spectroscopy versus the applied pressure.

Experimental Section

Synthesis Process. Compounds were prepared by solid-state reaction starting from Cu_2O , MoO_3 , and WO_3 . The reactants were ball milled thoroughly with acetone in a Syalon container with a Fritsch planetary instrument. The ball to powder weight ratio was fixed at 2:1, the rotational speed at 800 rpm, and the grinding duration at 1 h. These mechanically activated samples were then heated to 700 °C in air atmosphere for 24 h and then slowly cooled down to room temperature at about 5 °C min^{-1} .

Powder X-ray Diffraction. Powder X-ray powder diffraction patterns were recorded on a Philips PW 1820 apparatus equipped with a $\text{K}\alpha_1/\text{K}\alpha_2$ source. Diffraction patterns were collected with a 2θ step of 0.02° with a counting time of 10 s per step in routine mode or, for more advanced structural investigations, with a 2θ step of 0.015° with a counting time over 200 s per step. Diffractograms were refined via a Rietveld procedure^{10,11} using the FULLPROF program package. Unit cell parameters, atomic positions, atomic displacement parameters, and occupancy rates were refined and are summarized below.

Microscopy. Transmission electron microscopy (TEM) and scanning TEM (STEM) observations, as well as energy dispersive X-ray (EDX) experiments were performed using a JEOL 2200 FS equipped with a field emission gun, operating at 200 kV and with a point resolution of 0.23 nm.

Reflectivity Measurements. Diffuse reflectance spectra, $R(\lambda)$, were recorded at room temperature from 350 to 850 nm with a step of 1 nm and a band length of 2 nm on a Cary 17 spectrophotometer using an integration sphere. Halon was used as white reference for the blank. A mathematical treatment of the obtained spectra allowed the determination of the La^*b^* space

colorimetric parameters. The first step of the treatment consisted of obtaining the XYZ tri-stimulus values (defined by the CIE, 1964) from the integration (on the visible range, i.e. from $\lambda = 380$ nm up to 780 nm) of the product of $x(\lambda)$, $y(\lambda)$, or $z(\lambda)$ functions (CIE, 1964) with the diffuse reflectance spectra function: $X = \int x(\lambda) R(\lambda) d\lambda$. Then, the transfer equations defined by the CIE, 1976, from XYZ space to the La^*b^* space, were used to obtain the La^*b^* chromatic parameters. It was found that the transition $\alpha \rightarrow \gamma$ has a strong impact on the L (relative to the luminosity of the sample) and a^* (relative to the green-red axis of colorimetric space) parameters. Then, these two parameters were exploited to probe the $\alpha \rightarrow \gamma$ transition.⁸ For all the evolutions of L and a^* versus applied pressure, the curve was fitted by a Boltzmann sigmoidal function which may be written L or $a^* = A_2 + (A_1 - A_2)/(1 + e((P - P_0)/\Delta))$ where A_1 and A_2 are the value of the first and second plateau (dwelt), respectively, P_0 is the x -coordinate of inflection point, and Δ , in MPa^{-1} , is proportional to the slope of the curve at the inflection point (the linear curve which is tangent to the sigmoidal function on the inflection point gets the equation $y = (A_2 - A_1)/4\Delta$). Thus, for each oxide composition, the quantified transition pressure can be determined from this fit considering P_0 as the transition point.

For the characterization of the phase transition with temperature at ambient pressure, a home-built instrument equipped with a photomultiplier to collect the integrated reflected intensity in the 500–550 nm region (a green filter was employed) was used. The nitrogen cryostat allows measurement between 50 and 400 K with a heating and a cooling rate here roughly fixed at 5 K min^{-1} . The transition temperature was directly extracted from the total reflexivity evolution.

High Pressure Procedure. Pressure was applied using two different instruments:

- an ultrahigh hydrostatic pressure induced from oil media. To change the crystallographic parameters in an irreversible way in a few samples, powder was thermally sealed at 100 °C in a nonporous polyethylene hermetic bag (Cryovac-NOP-120) before it was carried out in an 80% vacuum to ensure that the minimum amount of air remains in the bag. The hyperbar experimental apparatus used was designed and produced by NFM-Technologies (Le Creusot, France) and Framatome (Paris, France) and marketed by CLEX-TRAL (Firminy, France). This apparatus is able to reach a maximal pressure of 0.8 GPa. Samples bags were hydrostatically pressed in a 3 L sample compartment at 0.7 GPa during 1 min at ambient temperature and with a pressure-climbing rate of 375 MPa per minute. Both pressure and temperature were constantly monitored and recorded during the process.

- a high hydrostatic pressure induced from oxygen gas. For characterization of the piezochromic pressures at room temperature, equipment able to reach pressures up to 5 kbar (500 MPa) is used, and several compression stages are performed. The selected pressure is obtained by compression of the oxygen gas from a bottle of oxygen (200 bar) inside specific reaction vessels in nickel alloys.

Results and Discussion

Influence of Tungsten Rate in $\text{CuMo}_{1-x}\text{W}_x\text{O}_4$ Oxides on Their Transition Pressures. It has been already shown in our previous publication⁸ that, although tungsten is substituted for molybdenum, the γ -form is stabilized at the expense of the α -form. Hence, the transition temperatures for both cooling or heating mode are raised by about 100 K going from CuMoO_4 to $\text{CuMo}_{0.9}\text{W}_{0.1}\text{O}_4$. By analogy, it appears clear that the tungsten rate may permit the control

(8) Rodríguez, F.; Hernandez, D.; Garcia-Jaca, J.; Ehrenberg, H.; Weitzel, H. *Phys. Rev. B* **2000**, *61*, 16497.

(9) Gaudon, M.; Carbonera, C.; Thiry, A. E.; Demourgues, A.; Deniard, P.; Létard, J. F.; Jobic, S. *Inorg. Chem.* **46**, **2007**, *24*, 10200–10207.

(10) Rietveld, H. M. *J. Appl. Crystallogr.* **1969**, *2*, 65–72.

(11) Rietveld, H. M. *Acta Crystallogr.* **1967**, *22*, 151–158.

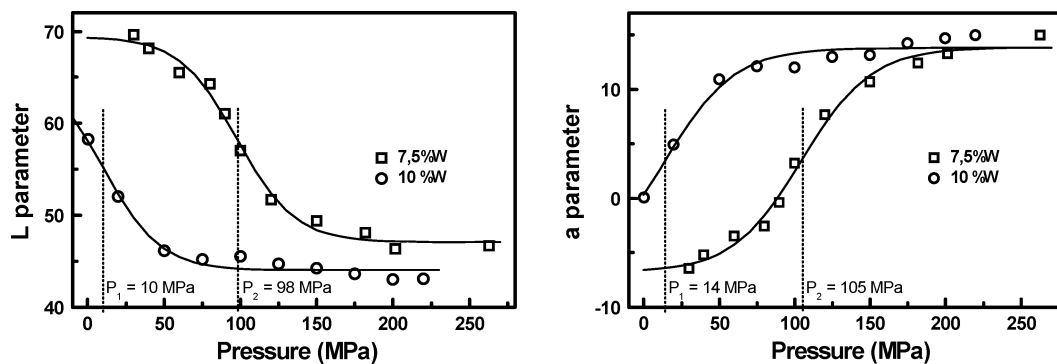


Figure 1. Evolution of L and a^* colorimetric parameters versus applied pressures at room temperature for two different $\text{CuMo}_{1-x}\text{W}_x\text{O}_4$ compositions (circles, $x = 0.1$, and squares, $x = 0.075$).

Table 1. Fit Parameters Obtained from the Different L and a^* Evolutions (1)

fit curve name	A_1	A_2	P_0 (MPa)	Δ (MPa^{-1})
L curve ($x = 0.075$)	69 ± 1	47 ± 1	98 ± 3	19 ± 3
a curve ($x = 0.075$)	-7 ± 1	14 ± 1	105 ± 4	23 ± 4
L curve ($x = 0.10$)	66 ± 1	44 ± 1	10 ± 2	19 ± 3
a curve ($x = 0.10$)	-7 ± 1	14 ± 1	14 ± 3	23 ± 4

of the $\alpha \rightarrow \gamma$ transition pressure. It was thus decided to characterize the $\alpha \rightarrow \gamma$ pressure transition by means of the reflectivity set-up after the release of the applied pressure (to follow the drastic change of the L and a^* colorimetric parameters); thus, these measurements are possible only for samples which can exhibit the two allotropic forms α and γ in pressure-temperature ambient conditions (i.e., $0.075 < x < 0.1$).

In Figure 1, the evolutions of the L and a^* colorimetric parameters versus the applied pressure on α -samples are reported for the two compositions: $\text{CuMo}_{0.925}\text{W}_{0.075}\text{O}_4$ and $\text{CuMo}_{0.9}\text{W}_{0.1}\text{O}_4$. First, one can notice that the extraction of the transition pressure either from the L curve or from the a^* curve leads to nonsignificant deviations (Table 1). For $x = 0.075$, the pressure transition is about 100 MPa, and for $x = 0.1$, this pressure is about 12 MPa (average value between the two transition pressures extracted from the L and a^* curves). The δx value, characteristic of the phase transformation speed, that is, the transition steepness versus pressure, is the same whatever the composition. The increase of the tungsten rate seems to modify only the transition pressure without changing the transition kinetics. The A_1 and A_2 values, which are respectively characteristic of the colorimetric parameter of the α -form and the γ -form, are identical from the two colorimetric parameter curves, so the experiment seems to be consistent (this also shows that the tungsten rate has a very slight influence on the α and γ modifications color).

In Figure 2, the evolution is given of the transition pressure versus tungsten concentration based on the aforementioned results and data reported in the literature. As it was evidenced for the transition temperature dependence versus W rate, the evolution of the pressure transition versus tungsten rate could be roughly considered as linear. The increase of the tungsten rate induces a linear decrease of the pressure transition (other compositions have to be studied to conclude definitively on the exact shape of the evolution curve). Therefore, the transition pressures are very tunable in a wide range of

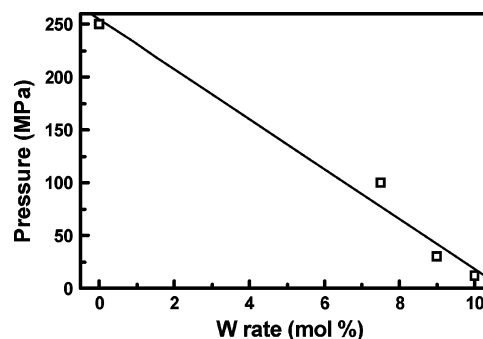


Figure 2. Evolution of the characteristic pressure transitions versus tungsten content.

pressures via the tungsten rate, and, in terms of industrial applications, the prepared material can be thus used as shock detectors for a large pallet of pressure (for example, in aerospace or building materials subjected to high constraints). Furthermore, it can be noticed that for the prepared powdered samples constituted of 1–50 μm diameter grains, the $\alpha \rightarrow \gamma$ transition can be easily triggered by application of a low pressure: the pressure of one finger push is all that is needed to transit from green to red at room temperature for the $\text{CuMo}_{0.9}\text{W}_{0.1}\text{O}_4$ sample, for instance. In consequence, one can deem that the synthesized materials can find applications in cosmetics or other domains.

Nevertheless, it has to be insisted that, for a defined chemical composition, the transition pressure is highly temperature sensitive. This claim is illustrated by the forthcoming study showing the large influence of the external temperature on the transition pressure of the $x = 0.09$ tungsten rate composition.

Influence of Temperature on $\text{CuMo}_{0.91}\text{W}_{0.09}\text{O}_4$ Transition Pressures. To highlight the strong dependence of the transition pressures with temperature, the colorimetric curves L and a^* parameters versus the applied pressures at 298 K and 323 K are reported in Figure 3 while results of the fitting are reported in Table 2. At room temperature (297 K), the transition pressure is about 30 MPa, and for the sample heated at 323 K, the transition pressure goes up to 160 MPa. An increase of 25 K is sufficient to multiply the transition pressure by a factor of about 5. The very important augmentation of the transition pressure for the same composition versus a slight increase of the temperature shows that, for a fixed pressure, the α -form is largely stabilized in

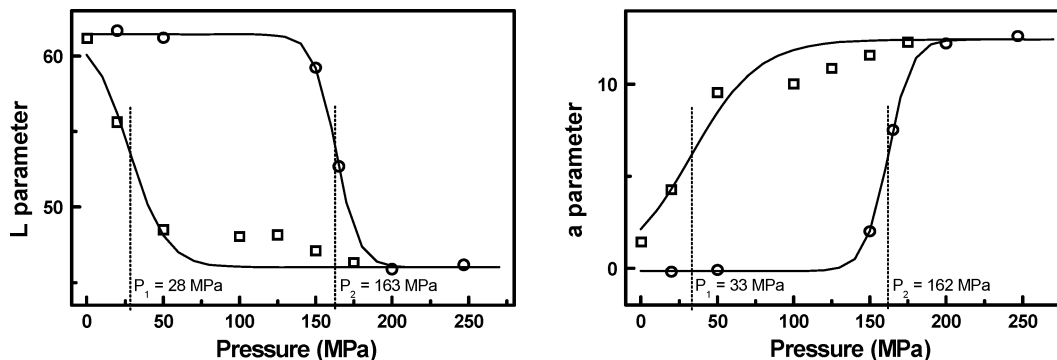


Figure 3. Evolution of L and a^* colorimetric parameters vs applied pressures on $\text{CuMo}_{0.91}\text{W}_{0.09}\text{O}_4$ composition at 298 K (squares) and 323 K (circles).

Table 2. Fit Parameters Obtained from the Different L and a^* Evolutions (2)

fit curve name	A_1	A_2	P_0 (MPa)	Δ (MPa^{-1})
L curve (298 K)	61 ± 1	46 ± 1	163 ± 3	7 ± 1
a curve (298 K)	0 ± 1	12 ± 1	162 ± 4	7 ± 1
L curve (323 K)	61 ± 1	47 ± 1	28 ± 5	12 ± 3
a curve (323 K)	0 ± 1	12 ± 1	33 ± 7	22 ± 7

warm conditions to the detriment of the γ -form. Elsewhere, the other parameters of the sigmoidal curve relative to the phase transition were analyzed. Concerning the asymptotic A_1 and A_2 values, no influence on temperature was detectable because of the aforementioned reasons in the last paragraph (weak influence of the temperature on the α or γ -forms color), but they differ concerning the δx transformation speed. For the sample studied at room temperature, δx is about 20 MPa^{-1} as it was determined for the compositions $x = 0.075$ and $x = 0.1$ studied at room temperature previously. Hence, this last manipulation confirms that the tungsten rate does not modify the transformation speed. For the heated sample at 323 K, δx becomes only about 7 MPa^{-1} and the transformation seeming “kinetically activated” and therefore more “brutal”. At this point of the study, this experiment seemed us consistent with a germination-growth mode for the phase transition. Indeed, by analogy with the formation of a precipitate inside a liquid media, one can think that the γ -form appears under pressure inside the α one by a nucleation mechanism followed by a growth of the so formed nuclei. The last experiment only indicates that the temperature seems to activate the kinetics of the germination-growth step of the γ -form inside the α -form host crystallites. Elsewhere, this experiment already puts in evidence that the first-order phase transition is P , T dependent in the sense that it can not be envisioned to study the influence of one parameter without clearly fixing the other one. Moreover, this study underlines the fact that this system is sensitive to a slight change in temperature which induces important modifications in the transition pressure; that could limit some of the applications or, conversely, can be used to create new P , T indicators generated for objects subjected to coupled high temperature and high pressure (in transport and energy devices, for example).

At the end, the important impact on the piezochromic or thermo-chromic properties of the thermal history and/or pressure history of the samples has been studied. This study

was again performed on the $x = 0.09$ tungsten rate composition, as previously.

Influence of the “Sample History” on $\text{CuMo}_{0.91}\text{W}_{0.09}\text{O}_4$ Transition Pressures/Temperatures. The temperature/pressure history of a sample can have a considerable impact on the first-order transition (P , T) parameters. Indeed, the phase transition, which is accompanied by a strong change of volume of the crystallographic cell, is accompanied by atomic displacements because, at the transition, a coordination change of the metallic cations occurs. Thus, one can suppose that the more the temperature/pressure on both sides moves away from the phase transition point, the more the α - γ crystallographic networks differ. Two simultaneous effects can be inferred: (1) dilatation/contraction of the cell and (2) atomic migration. A priori, the thermal history of the sample—quenching, high pressing—should have an important influence on the transition pressures/temperatures if this history allows (a least partially) the atomic positions to be fixed. The first study compared the characterized transition pressures between an α phase quenched from $700 \text{ }^\circ\text{C}$ and another one slowly cooled down until room temperature (in standard conditions). The second study, in a reciprocal way, dealt with the influence of the preliminary application on γ -form of a very high pressure (5 kbar) on the $\gamma \rightarrow \alpha$ transition temperature.

In Figure 4, the L and a^* parameter curves are depicted versus applied pressure for the determination of the $\alpha \rightarrow \gamma$ transition pressures for samples quenched in air or samples cooled at $5 \text{ }^\circ\text{C/h}$. To fit the colorimetric parameter curves for the quenched sample, because of the domain of characterization was not extended enough to obtain the complete S curve, the A_2 parameter (second dwelt of the S) has been fixed as equal to that of the standard sample, considering that in both cases the L or a parameter then correspond to a 100% γ -form and do not differ from one sample to another. The fit results which are reported in Table 3 clearly show the strong impact of the quenching on the transition pressure. Indeed, the transition pressure of this compound is five times more important than the one determined of the standard one. Furthermore, the quenching seems to have a considerable effect on the transition kinetics, making it here softer. Therefore, this experiment clearly proves that the phase transformation is due to atomic migrations and not only a dilatation effect because dilatation is avoided as well by a slow cooling down or by a quenching.

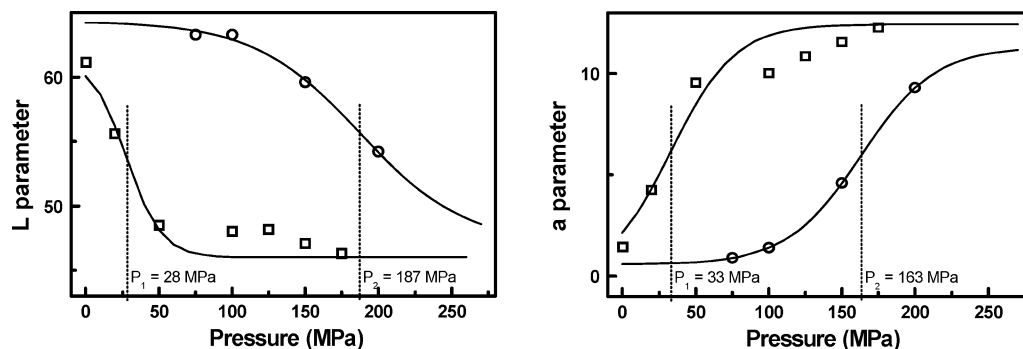


Figure 4. Evolution of L and a^* colorimetric parameters vs applied pressures of $\text{CuMo}_{0.91}\text{W}_{0.09}\text{O}_4$ composition obtained (a) from standard thermal process (squares) and (b) quenched from 700 °C (circles).

Table 3. Fit Parameters Obtained from the Different L and a^* Evolutions (3)

fit curve name	A_1	A_2	P_0 (MPa)	Δ (MPa^{-1})
L curve (quenched)	64 ± 1	47	187 ± 6	36 ± 7
a curve (quenched)	1 ± 1	12 ± 1	163 ± 1	25 ± 1
L curve (standard)	61 ± 1	47 ± 1	28 ± 5	12 ± 4
a curve (standard)	0 ± 1	12 ± 1	33 ± 7	22 ± 7

In Figure 5, reflectivity measurements are reported versus temperature of the high pressed γ sample. Three half-cycles were performed on the sample—half-cycles 1 and 3 corresponding to a heating ramp, half-cycle 2 corresponding to a cooling one—to compare the eventual effect of the “pressure” history between half-cycle 1 and 3. These three half-cycles have been fitted in a same way as previously by a sigmoidal curve (Table 4), the transition temperature being estimated at the inflection point of the curve at the heating. The transition temperature was calculated to be at about 384 K for the first half-cycle and about 370 K for the third half-cycle; this shows the loss of the overpressing influence. So, the transition temperature of the over pressed phase seems shifted toward slightly higher values which produces, of course, a stabilization of the high pressure form with a very high pressing per analogy with the stabilization of the high temperature form with a quenching. Nevertheless, the effect on transition pressure is very slight in comparison to that of quenching.

In the last parts, the differences between the quenched and the slowly cooled α -form from a structural and a chemical composition (on a microscopic level) point of view were investigated in regard of the γ -form. The structural difference was first investigated by X-ray analyses; local chemical composition, second, was done using TEM.

Structural Investigation of A Forms Phase Transition.

On a structural point of view, the difference between quenched and slowly cooled down phase was explained on the basis of the hypothesis of discrimination from local atomic positions inside the cell. The idea is to show which atomic migrations are at the origin of the “stabilization effect” that occurred from the quenching since the $\alpha \rightarrow \gamma$ transition pressure is then shifted toward some higher values. For this study, cell parameters, atomic positions, and isotropic displacement factors were calculated from the X-ray patterns on the various forms investigated: slowly cooled α -form, quenched α -form, and quenched γ -form (the complete set of structural data as well as graphical illustrations are found

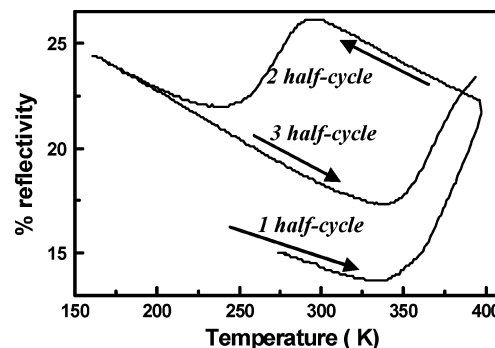


Figure 5. Evolution of the total percent of reflectivity in the green zone (500–550 nm) of $\text{CuMo}_{0.91}\text{W}_{0.09}\text{O}_4$ compound with temperature of the (a) unpressed sample and (b) pressed sample.

Table 4. Fit Parameters Obtained from the Different Reflectivity Half-Cycles

fit curve name	A_1	A_2	T_0 (K)	Δ (K^{-1})
1st half-cycle	17.2 ± 0.1	23.7 ± 0.1	370.2 ± 0.3	9.2 ± 0.37
3rd half-cycle	13.5 ± 0.1	24.3 ± 0.3	383.9 ± 0.8	13.2 ± 0.4

in the Supporting Information Tables S1, S2, and S3 and Figures S1 and S2. The patterns obtained for the three investigated forms show both samples were purely phases. Several points from the Rietveld refinement results have to be discussed. First, it has to be said that even if the very high number of parameters to refine appears inconvenient, it seems to be largely compensated by the large quantity of information provided by the diffraction pattern (large quantity of diffraction peaks); the correlation factors are rather good: R_{Bragg} values are about 8–9%. In the same way, it has been checked that the modification of the atomic position of one ligand has considerable repercussions on the refinement quality. Second, the quenching has logically no effect on cell volume, the dilatation being due to asymmetrical atomic vibration directly linked with the temperature. More surprisingly, the quenched and standard α -forms also present both the same cell parameters ratio and roughly the same atomic positions in respect to the γ -form. Indeed, the only explanation of the “stabilization” of the quenched α -form envisaged until now was that of atomic migrations making the quenched α -form farther from the γ -form than the standard α -phase, as previously explained. Thus, one can think that the atomic positions of the standard α -form should be intermediate to the atomic positions of the quenched α -form and the γ -form. Actually, there is no significant change between the two α -forms versus thermal

history of W rate as well on the cell parameters (a , b , c , α , β , γ), on atomic positions, on the various bond distances, and so forth. Hence, the very slight differences observed between the two differently synthesized α - and γ -forms are negligible in comparison with the atomic migrations generated by the phase transition from α toward γ .

The phase transition is a reconstructive (with a change of some cation coordination spheres) and a first-order (with a drastic change of volume during the transition⁵) phase transition. The transition mode should be a priori a germination-growth mode. Nevertheless, in all cases, it can be thanked that, because the atomic migrations are indubitably the source of the phase transition, these migrations can be followed and studied with X-ray diffraction. At this point of the study, only one explanation can be formulated: the global average migrations are negligible. However, this phenomenon could mask local disorders more and, more importantly, inside the two phases while the proximity to the transition phase point increases. Indeed, between the refinements of the quenched and the standard α -forms, a significant difference is observed between their isotropic displacement factors. The B_{iso} (\AA^2) values are more intense in the standard form than in the quenched one: 0.70(2), 0.73(3), and 1.52(8) for the standard form; 1.19(1), 1.53(7), and 2.67(8) for the quenched form and the Cu, Mo, and O sites, respectively. This large difference cannot be explained by the atomic agitation, the two X-ray spectra being recorded at same temperature. Surely, the augmentation of the displacement factors between the quenched and the standard form produces the fact that the quenched phase was stabilized compared to the standard one, leading to a relaxation of the local constraints occurring after the phase transition and to a decrease of the local atomic disorder. Hence, the real motor of the future different behavior, besides transition pressure needed to make the α - γ transition between the quenched and the standard α phases, may be attributed to local disorder, a notion normally only involved in second-order phase transition types. All this happens as the first-order transition is preceded and triggered by a “second order transition”, associated with continuous and cooperative atomic disordering. More detailed analyses of the phase transition mechanism are currently under investigation to confirm or deny the proposed hypotheses.

Chemical Composition of A Forms Phase Transition.

It can also be thought that the phase transition temperatures of the quenched and slowly cooled down α -forms differ because the Mo and W distributions are most probably not homogeneous in the samples. Indeed, segregations can come from further reasons: (i) they are the result of a nonachieved solid state reaction, (ii) they can occur during the cooling state, and (iii) more probably, they can be generated from a high surface affinity of one of the atoms. This important aspect has not been yet considered, and furthermore, this point was already raised for the $\text{Cu}(\text{W},\text{Mo})\text{O}_4$ systems, although for W-rich compositions with wolframite-type structure.¹²

TEM investigations were performed on some α -form grains to try to detect a segregation of tungsten in the

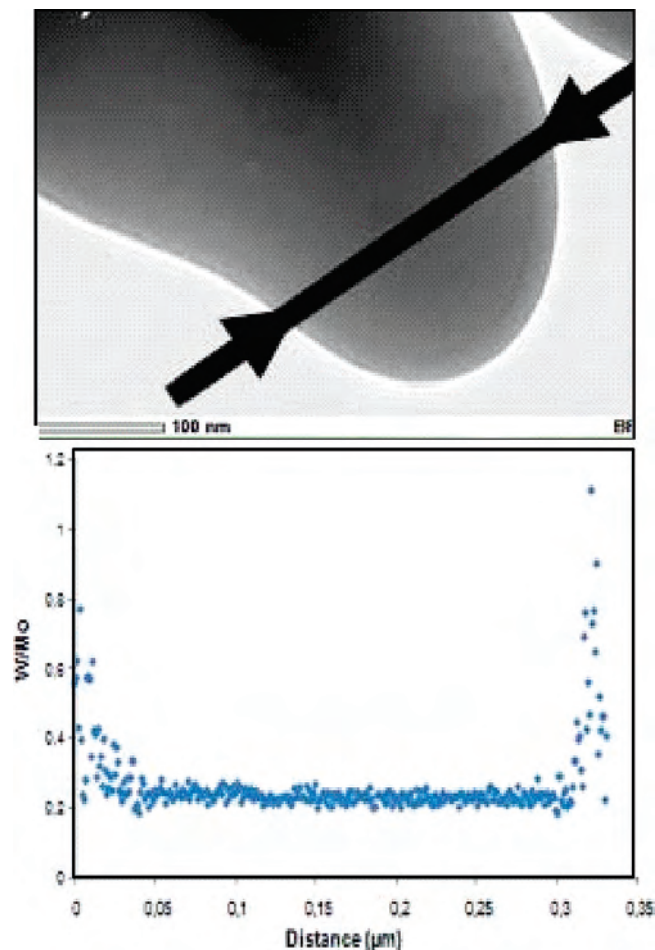


Figure 6. TEM micrograph of an α -form grain (quenched sample) and W/Mo ratio profile (made on the indicated segment by EDX).

quenched form compared to the slowly cooled down form. It is difficult to put on evidence that the tungsten is initially segregated, the two samples exhibiting the same behavior (quenched or slowly cooled sample). Nevertheless, it was shown that when the sample is submitted to the probe, the tungsten distribution becomes more and more segregated at the grains boundaries. This effect is brought to the fore on the EDX profile analysis reported on the Figure 6. The segregation under the probe is without any doubt caused by the reducing conditions associated to the probe (after very long time of acquisition, a demixtion of the sample in Mo–W-rich oxides and metallic copper is observed). Hence, this study has shown that one can think that there is a large possibility for a tungsten segregation to be at the origin of the transition temperatures difference between quenched and slowly cooled down forms. Indeed, high temperature acts as a more “reductive atmosphere” than room temperature, and the quenched sample probably exhibits a slight surface tungsten segregation. It can be added here that the tungsten may be segregated because it is the “substituting dopant” and is subjected to large constraints in the bulk matrix.

(12) Ehrenberg, H.; Theissmann, R.; Gassenbauer, Y.; Knapp, M.; Wltschek, G.; Weitzel, H.; Fuess, H.; Herrmannsdorfer, T.; Sheptyakov, D. *J. Phys.: Condens. Matter* **2002**, 8573.

Conclusion

CuMo_{1-x}W_xO₄ series with $x \leq 0.1$ are piezochromic materials with a transition pressure that can be tuned in an extraordinarily large range depending on the value of x (from a few to many hundred mega pascals). The important optical contrast between the two polymorphic phases and the fact that for some members of the series the pressure of one finger push is all that is needed to transit from green to red at room temperature can open up various applications for these materials as shock detectors. Nevertheless, in this study, one evidence is that external temperature and thermal history (quenched or not) of the samples influence significantly the transition pressure too. The origin of the sample thermal history was not perfectly assessed, but two different hypotheses can be formulated. Firstly, the accurate study of the structural evolution of the two polymorphic phases on both

sides of the transition pressure has highlighted that the first-order transition is triggered by an atomic disordering and is not accompanied by atomic migrations; this atomic disordering may be the cause of the sample history influence. Moreover, TEM-EDX investigations have shown that reductive conditions favor tungsten segregation at the grain boundaries, and one can then wonder why the quenched sample exhibits slight tungsten segregation. Finally, it can be thought that the local atomic disorder is well linked to the spatial W gradient from the bulk through to the surface of the grains.

Supporting Information Available: Two figures with illustrations of X-ray data and Mo₂ atomic migration and three tables with Rietveld refinements (PDF). This material is available free of charge via the Internet at <http://pubs.acs.org>.

IC702282T